

Open-chain and cyclic amidrazones forming persistent radicals. An electrochemical and quantum chemical study

Fabian Krauth,^{a*} Rudolf Friedemann,^b Hans-Hermann Rüttinger,^a and Petra Frohberg^a

^a Institute of Pharmacy, Martin-Luther-University Halle-Wittenberg
Wolfgang-Langenbeck-Str. 4, D-06120 Halle, Germany

^b Institute of Chemistry, Martin-Luther-University Halle-Wittenberg,
Kurt-Mothes-Straße 2, D-06120 Halle, Germany
E-mail: fabian.krauth@pharmazie.uni-halle.de

Abstract

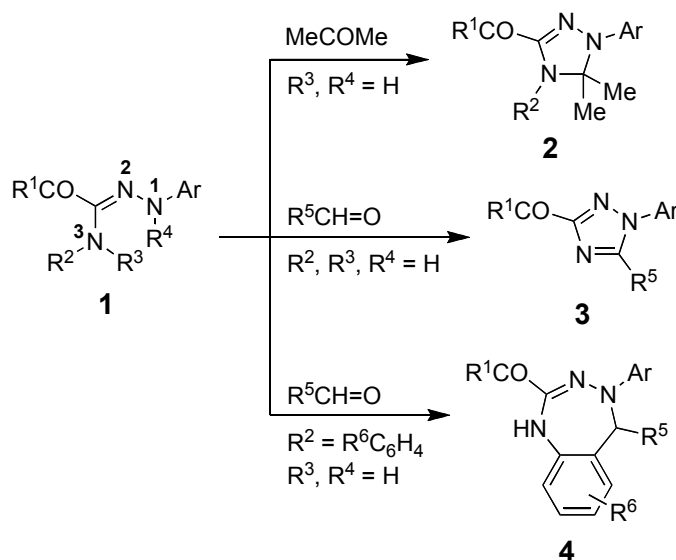
The electrochemical oxidation of various open-chain and cyclic amidrazones in acetonitrile was investigated by cyclic voltammetry. The oxidation was found reversible for both N^2 -disubstituted open-chain amidrazones and all cyclic compounds with the exception of triazole derivatives that could not be oxidized. Microcoulometry revealed an extrapolated charge consumption of one electron per molecule. The experimentally obtained oxidation potentials correlate well with the reaction energy of oxidation calculated from density function theory (DFT) that clearly supports the hypothesis of a persistent radical formation. The total atomic spin density of radical cations was calculated and permits to make a statement about the localization of radical formation. The synthesis of (*E*)-2-(methylphenyl)hydrazono-*N*-phenyl-2-piperidin-1-ylacetamide **7** representing open-chain α -carbonyl substituted N^2 -alkyl, aryl-amidrazones and the synthesis of 6-amino-substituted 2,3,4,5-tetrahydro-1,2,4-triazin-5-ones, a new class of amidrazones, are described.

Keywords: Cyclic voltammetry, amidrazones, 1,2,4-triazin-5-ones, density function theory, persistent radicals

Introduction

Amidrazones **1** are known as convenient building blocks for various N-heterocycles, such as 4,5-dihydro-1*H*-1,2,4-triazoles (triazolines) **2**, 1*H*-1,2,4-triazoles **3**, or benzotriazepines **4** (Scheme 1).¹ In recent years, various biological activities have been discovered for amidrazone compounds, e.g., fungistatic², bacteriostatic, and antimycotic³ activities as well as inhibitory effects on mammalian and plant enzymes, e.g. lipoxygenases (LOX)⁴ that are possibly subject to a redox mechanism.

The aim of our study is: (i) To evaluate the redox behavior of compounds that belong to different classes of amidrazones⁵ (Scheme 1, Tables 1–5) with structural and substituent variations; for this purpose, cyclic voltammetry in an aprotic medium was successfully applied. (ii) To gain further insight into the nature of the oxidation products we used density function theory (DFT) calculations on the B3LYP/6-31G(d) level⁶ that allows not only to localize the main spin density of the radical cation, but also provides information about geometrical changes of the molecule during the oxidation process. The results are expected to make a contribution to elucidate the amenability of amidrazone compounds for participation in redox processes and to make a first statement about the most likely mechanism of persistent amidrazone radical formation.⁷



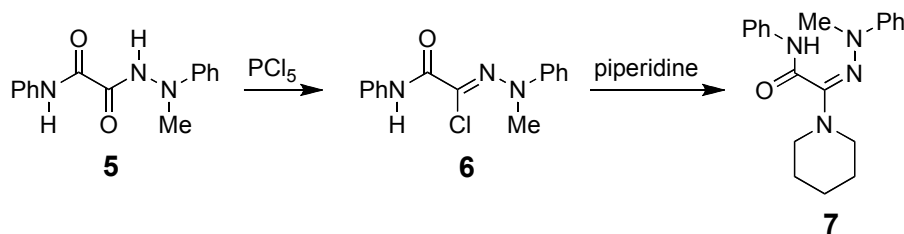
Scheme 1. IUPAC nomenclature numbers the distant nitrogen atoms of the amidrazone skeleton N1–C=N–N2 only. Contrary, we use the numbering as shown for **1** in order to apply consistent numbering as used in previous publications.⁵ For substituents in **1–4** see Table 1 and Tables 3–5.

Additionally, we exemplify the synthesis of open-chain α -carbonyl substituted N^2 -alkyl, aryl-amidrazones and 6-amino-substituted 2,3,4,5-tetrahydro-1,2,4-triazin-5-ones as cyclic compounds with amidrazone scaffold. Substituents and oxidation potentials are presented in Tables 1–5. Cyclic voltammograms showing the formation of persistent radical cations are provided and results of quantum chemical calculations are related to the electrochemical data.

Results and Discussion

Synthesis

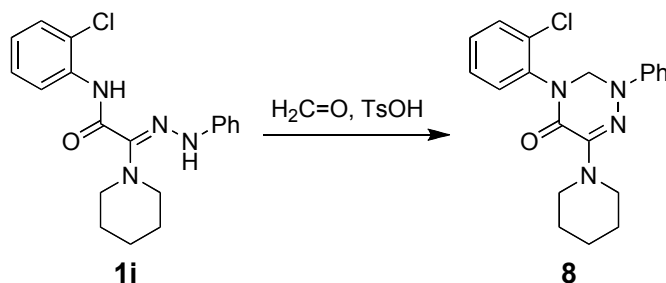
Hydrazonoyl chlorides as starting compounds for N1-disubstituted open-chain amidrazones could not be prepared via the generally applied Japp-Klingemann cleavage. Therefore, an alternative synthetic pathway had to be explored. In the literature, a number of different strategies have been reported.⁸ For our purpose, (*Z*)-*N*-methyl-*N*-phenylhydrazonoyl chloride **6** was obtained by the reaction of oxanilide *N*-methyl-*N*-phenylhydrazide **5** with phosphorus pentachloride according to a reported procedure.⁹ The hydrazonoyl chloride **6** was subsequently converted into amidrazone **7** by the reaction with piperidine (Scheme 2).



Scheme 2

Using NOE experiments, **7** was found to exist as *E* isomer unlike the reported N1-mono-substituted amidrazones such as **1i**⁵ (Scheme 3). Irradiation at the frequency of the methyl protons causes an NOE to CONH but not to NCH₂ of the piperidine ring.

To investigate the mechanism of cyclization, which results in benzotriazepines, triazoles and triazolines, we chose not only N3-unsubstituted amidrazones as starting materials but also N3-mono- and disubstituted amidrazone derivatives (Scheme 1, Table 1). Reaction of amidrazone **1i** with formaldehyde in the presence of *p*-toluenesulfonic acid yielded a product which was identified as compound **8** (Scheme 3), the first member of a novel cyclic amidrazone class of 6-amino-substituted 2,3,4,5-tetrahydro-1,2,4-triazin-5-ones.



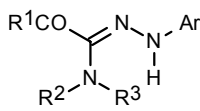
Scheme 3

In the NMR spectra, a long-range coupling was observed between both protons in position 3 of the triazinone ring and the aromatic carbons directly bonded to the nitrogen atoms in triazinone positions 2 and 4. Electron impact mass spectrometry (EI-MS) and results of elemental analysis confirm the constitution of this structure.

Electrochemistry

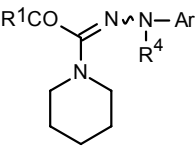
Owing to their hydrazone structure, all amidrazones are susceptible to oxidation. Some of these species having a very low oxidation potential, such as (*E*)-**1p** or (*E*)-**1q** (Table 2), are readily oxidized in diluted solutions (in DMF, MeOH or MeCN) as soon as they are exposed to air. This autoxidation process results in highly colored solutions from the original colorless compounds, and in most cases hydrogen peroxide can be found as reduction product of molecular oxygen. In order to gain further insight into the oxidation process we determined the electrochemical oxidation potentials of all the amidrazones comprised in Tables 1–5 by cyclic voltammetry at a platinum microelectrode. To avoid complications by reactions prior to electrochemical oxidation and immediate decomposition of the oxidation products, acetonitrile was used as an inert solvent.

Table 1. Oxidation potentials of open-chain N1-monosubstituted amidrazones (*Z*)-**1a–o**

	R ¹	Ar	R ² /R ³	Oxidation potential ^a
1a ^b	PhNH	Ph	H/H	740 mV
1b	PhNH	Ph	CH ₃ /H	560 mV
1c	PhNH	Ph	Ph/H	790 mV
1d	PhNH	3-FC ₆ H ₄	H/H	840 mV
1e	PhNH	4-CH ₃ C ₆ H ₄	CH ₃ /H	520 mV
1f	PhNH	4-ClC ₆ H ₄	CH ₃ /H	600 mV
1g	2-ClC ₆ H ₄ NH	Ph	CH ₃ /CH ₃	710 mV
1h	2-ClC ₆ H ₄ NH	Ph	4-ClC ₆ H ₄ /H	880 mV
1i	2-ClC ₆ H ₄ NH	Ph	(CH ₂) ₅	720 mV
1j	2-ClC ₆ H ₄ NH	2-ClC ₆ H ₄	H/H	800 mV
1k	2-ClC ₆ H ₄ NH	3-ClC ₆ H ₄	CH ₃ /CH ₃	720 mV
1l	3-ClC ₆ H ₄ NH	3-ClC ₆ H ₄	H/H	730 mV
1m	4-FC ₆ H ₄ NH	3-CH ₃ COC ₆ H ₄	H/H	680 mV
1n	CH ₃ CH ₂ O	4-ClC ₆ H ₄	H/H	760 mV
1o	CH ₃ OCO(CH ₂) ₃	Ph	Ph/H	900 mV

^aElectrochemical oxidation of all compounds **1a–o** was irreversible. ^bAvailable as hydrochloride.

Table 2. Oxidation potentials of N1-monosubstituted reference amidrazones **1p**, **1q**, and N1-disubstituted amidrazone **7**

	R ¹	Ar	R ⁴	oxidation potential ^a
(<i>Z</i>)- 1p	PhNH	Ph	H	720 mV
(<i>E</i>)- 1p	PhNH	Ph	H	470 mV
(<i>E</i>)- 1q ^b	(CH ₃) ₂ N	4-CH ₃ C ₆ H ₄	H	330 mV
(<i>E</i>)- 7	PhNH	Ph	CH ₃	580 mV

^aElectrochemical oxidation of **1p** and **1q** was irreversible, **7** reversible. ^b(*Z*)-**1q** could not be prepared.

Table 3. Oxidation potentials of the triazolines **2a–i**

Compound	R ¹	Ar	R ²	Oxidation potential ^a
2a	PhNH	Ph	H	640 mV
2b	PhNH	Ph	CH ₃	570 mV
2c	PhNH	3-FC ₆ H ₄	H	730 mV
2d	PhNH	4-CH ₃ C ₆ H ₄	CH ₃	490 mV
2e	PhNH	4-ClC ₆ H ₄	CH ₃	580 mV
2f	2-ClC ₆ H ₄ NH	Ph	H	630 mV
2g	2-ClC ₆ H ₄ NH	3-ClC ₆ H ₄	H	770 mV
2h	3-ClC ₆ H ₄ NH	3-ClC ₆ H ₄	H	730 mV
2i	4-FC ₆ H ₄ NH	3-CH ₃ COC ₆ H ₄	H	680 mV

^a Electrochemical oxidation of all compounds **2a–i** was reversible.

Table 4. Oxidation potentials of triazoles **3a–c**

Compound	R ¹	Ar	R ⁵	Oxidation potential ^a
3a	2-ClC ₆ H ₄ NH	2-ClC ₆ H ₄	H	–
3b	CH ₃ CH ₂ O	4-ClC ₆ H ₄	H	–
3c	CH ₃ CH ₂ O	4-ClC ₆ H ₄	CH ₃	–

^aTriazoles **3a–c** were not amenable for electrochemical oxidation.

Table 5. Oxidation potentials of the benzotriazepines **4a–h**

Compound	R ¹	Ar	R ⁵	R ⁶	Oxidation potential ^a
4a	PhNH	Ph	Ph	–	710 mV
4b	2-Cl-C ₆ H ₄ NH	Ph	H	7-Cl	770 mV
4c	CH ₃ OCO(CH ₂) ₃	Ph	H	–	690 mV
4d	CH ₃ OCO(CH ₂) ₃	Ph	Ph	–	750 mV
4e	CH ₃ OCO(CH ₂) ₃	Ph	H	9- CH ₂ OH	670 mV
4f	CH ₃ OCO(CH ₂) ₃	Ph	H	7-Cl	730 mV
4g	CH ₃ OCO(CH ₂) ₃	4-ClC ₆ H ₄	H	–	740 mV
4h	CH ₃ OCO(CH ₂) ₃	4-ClC ₆ H ₄	H	7-Cl	800 mV

^a Electrochemical oxidation of all compounds **4a–h** was reversible.

The potentials were measured against a saturated Ag/AgCl reference electrode and corrected in reference to the oxidation potential of ferrocene. Open chain as well as cyclic amidrazones can be oxidized between 300 and 800 mV at the platinum electrode as shown exemplarily in Tables 1–3 and 5. Compound **8** (not mentioned in Tables 1–5 exhibits an oxidation potential of 658 mV. The aromatic triazoles **3a–c** (Table 4) demonstrated stability against electrochemical oxidation up to the limit of 1300 mV. Generally, the substitution pattern of the aromatic group (Ar) was recognized as an important structural aspect for the oxidation potential in all of the tested compound classes. Exemplified for the triazolines, it is apparent that electron withdrawing or rather electron releasing groups influence the potential to be oxidized. Substituents containing strong negative inductive effects, e.g., fluorine **2c** or chlorine **2e** atoms raise the required oxidation potential whereas unsubstituted **2b** or methyl-substituted **2d** phenyl groups support lower oxidation potentials. The voltammograms at the microelectrode show a typical sigmoid shape (see Figure 1) attributed to the special diffusion conditions at microelectrodes. Analysis gives a hint to a diffusion controlled one-electron step. This is confirmed by microcoulometry (see below). Open-chain amidrazones, which tend to form *E/Z* isomers, can additionally be qualitatively checked for impurities with the respective other isomer by cyclic voltammetry at a platinum microelectrode (Figure 1).

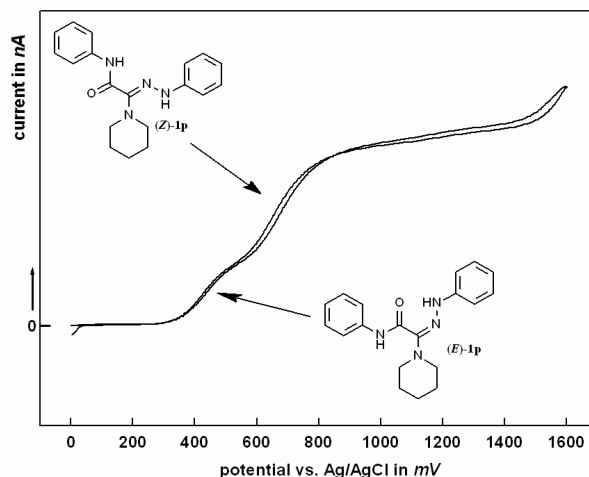


Figure 1. Cyclic voltammogram of **1p** [(Z:E) 2:1]; scan rate of 40 mV s^{-1} at a Pt microelectrode (d: 0.01 mm).

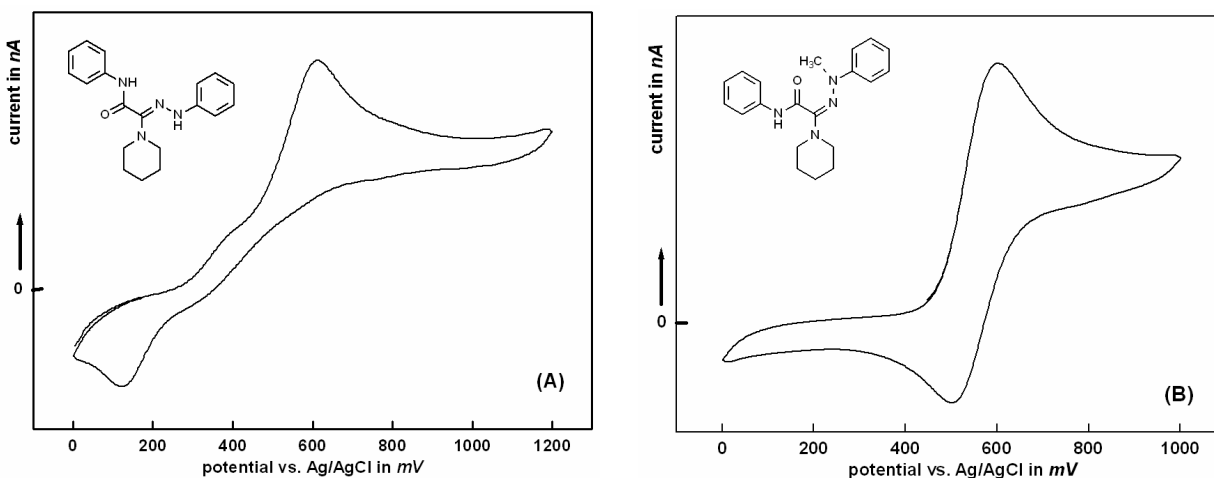


Figure 2. Cyclic voltammograms of (Z)-**1p** (A) and (E)-**7** (B) at a Pt macroelectrode (d: 0.15 mm) at a scan rate of 40 mV s^{-1} .

Both isomers (*E*)-**1p** and (*Z*)-**1p** exhibit a characteristic curve for an irreversible redox process at the macroelectrode like the other open-chain amidrazones with monosubstituted N1 ($R^4 = \text{H}$) (Figure 2A, (*E*)-**1p** not shown). Substitution of the N1-bonded hydrogen with e.g., a methyl group like in compound **7** leads to the appearance of a reversible intermediate radical species, as is readily evident from the shape of the cyclic voltammogram (Figure 2B) which correlates well with that of ferrocene. This radical state was found to be persistent for at least six repeated cyclovoltametric runs and beyond.

Similarly, the radical species of the triazolines, benzotriazepines and the novel triazinone compound **8** demonstrate a remarkable stability. The reversible behavior is shown for compound **2b** (Figure 3A) as an example for a triazoline and compound **8** (Figure 3B).

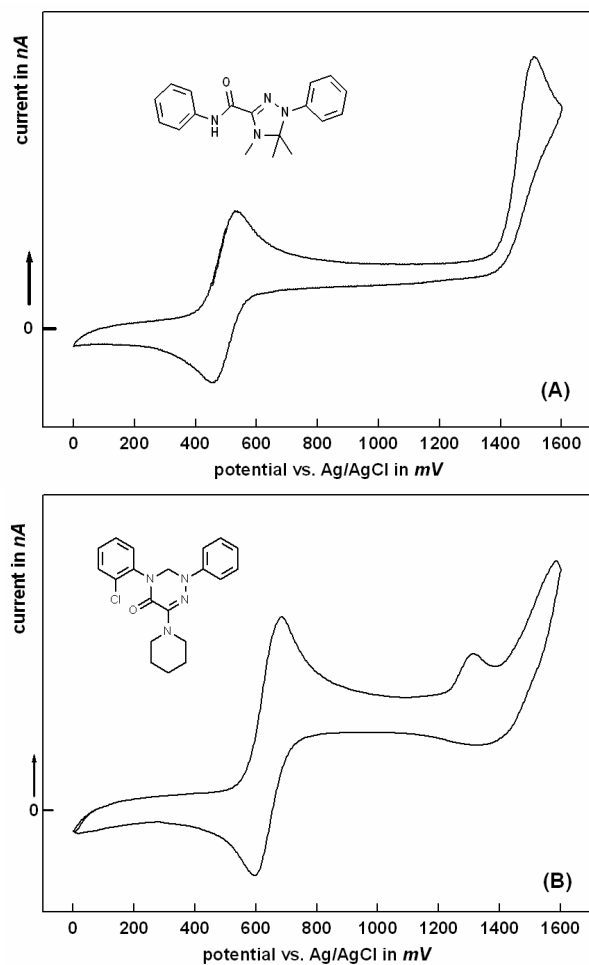


Figure 3. Cyclic voltammograms of **2b** (A) and **8** (B) at a Pt macroelectrode (d: 0.15 mm) at a scan rate of 40 mV s^{-1} .

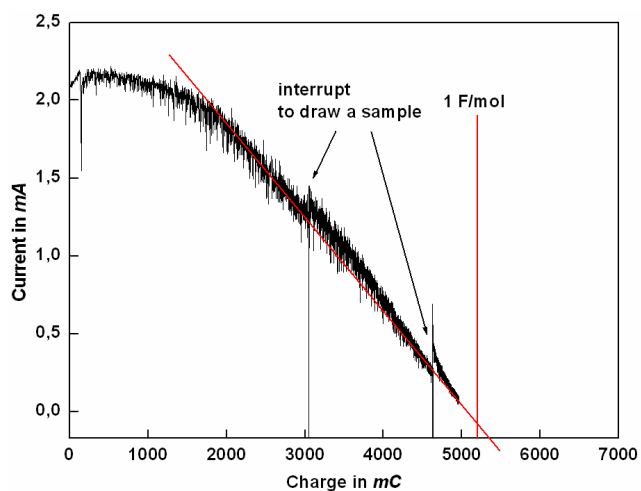


Figure 4. Preparative scale electrolysis of a solution containing $54 \mu\text{M}$ of **2d**.

Extrapolation of the electrolysis current results in a charge of 5.33 C corresponding to 1.02 electrons per molecule. The deviation of the current from linearity at the beginning of the electrolysis is attributed to the ohmic drop in the cell and does not compromise the result.

Microcoulometric oxidation of **2d** at a platinum sheet as the working electrode at 700 mV resulted in an extrapolated charge consumption of just one electron/molecule and yielded a stable deep green-blue colored solution that could be reduced at -200 mV to the starting compound (Figure 4). EPR spectra of the oxidized amidrazones clearly identify the product as a radical, however the spectra showed no fine structure, hence no information on the spin distribution could be obtained (data not shown). For gaining insight into the structures of the reaction products we used quantum chemical calculations.

Quantum chemical studies

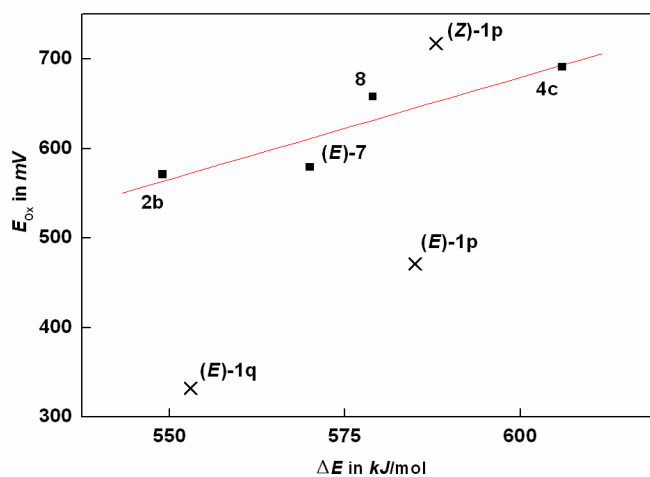
Density functional theory (DFT) calculations on the B3LYP/6-31G(d) level were performed on amidrazones and their radical cations to study structure-property relationships within the oxidation process of such compounds. The investigations were carried out on the isolated systems using the GAUSSIAN98 program package.⁶ The energetically preferred conformations of the neutral molecules and the radical cations were obtained by full optimization. The structures of the minima were characterized by frequency calculations on the same level. For molecules with an open amidrazone structure the possible *E* and *Z* isomers related to the C1-N2 double bond (for numbering see Figure 6) were taken as alternative starting structures to find the most stable conformers. Both amidrazones with a mono- and disubstituted N1 atom were considered as they show differences in their electrochemical oxidation behavior. The reaction energy ΔE of the amidrazones for the oxidation in the gas phase $A \rightarrow A^{\bullet+} + e^-$ was calculated. The obtained ΔE values were correlated with electrochemically measured oxidation potentials E_{ox} . In the electrochemical measurements the same solvent and similar conditions were used. Therefore, the measured E_{ox} data and the calculated ΔE values can be compared in some way. Within the more qualitative considerations we have not included thermal corrections and solvation effects. Moreover, the energy of the highest occupied molecular orbital ϵ_{HOMO} for the amidrazones was considered. The results are shown in Table 6. Amidrazones are classified with respect to the substitution at the N1 atom. The first part contains disubstituted compounds and the second part the monosubstituted ones.

Table 6. Calculated DFT reaction energies (ΔE), orbital energies (ϵ_{HOMO}) and electrochemically measured oxidation potentials (E_{ox}) for some amidrazones including (*E*) and (*Z*) isomers

Compound	ΔE (kJ/mol) ^a	ϵ_{HOMO} (eV) ^b	E_{ox} (mV) ^c
(<i>E</i>)-7	570	-4.82	580
2b	549	-4.95	570
4c	606	-5.06	690
3c	782	-6.75	-
8	579	-4.99	660
(<i>E</i>)-1p	585	-5.05	470
(<i>Z</i>)-1p	588	-5.35	720
(<i>E</i>)-1q	553	-4.67	330

^aReaction energy for the formation of the radical cation $A \rightarrow A^{\bullet+} + e^-$. ^bEnergy of the highest occupied molecular orbital in the neutral molecule. ^cElectrochemically measured oxidation potential for the oxidation process.

A correlation of the reaction energies ΔE with the oxidation potentials E_{ox} indicates that a certain relationship can only be found within the disubstituted compounds. This is illustrated in Figure 5. The calculated values for the compound **3c** (Table 6) are in qualitative agreement with the experimental findings of the difficult oxidability of such substances. The compounds with an N1-H bond (marked \times) in Figure 5 show significant deviations from the linear fit obtained by the systems with two substituents at the N1 atom. The results support the electrochemical findings that the presence of an N1-H function in the amidrazones causes an irreversible pathway of the oxidation process. Obviously, amidrazones with a N1-H bond show a more complex mechanism in the radical oxidation reaction.

**Figure 5.** Correlation between oxidation potentials E_{ox} and calculated reaction energies ΔE for the formation of the radical cations of disubstituted compounds **2b**, **4c**, (*E*)-7, **8** (■);

$y = -687.25 + 2.28x$; $r = 0.9105$. Monosubstituted compounds (*E*)-**1p**, (*Z*)-**1p**, and (*E*)-**1q** (\times) shows significant deviations from linear fit.

A comparison of the most stable conformers of the molecule and the corresponding radical cation indicates significant structural changes between the starting compound and the product of the oxidation reaction. This can be deduced from the energetically preferred structures of (*E*)-**1p** and its radical cation given in Figure 6. The molecular segments at the central C1 atom show a different arrangement in both species. It is remarkable that the formation of the radical cation causes a balance in the bond lengths of the amidrazone skeleton. Generally, in the radical cation the C1–N2 bond is lengthened and the C1–N3 bond is shortened in comparison to the corresponding neutral molecule. It is noteworthy that the bond lengths of the amidrazone skeleton for all of the calculated molecules are within the range, which was found in other amidrazone derivatives by X-ray measurements (1.30–1.37 Å for N1–N2, 1.28–1.30 Å for C1–N2 and 1.36–1.47 Å for C1–C3).^{4,5}

Intramolecular hydrogen bonds are relevant both in the most stable conformers of the amidrazones and their radicals but especially in the systems with an N1–H bond. It should be mentioned that there is no correlation between ϵ_{HOMO} and E_{ox} values (Table 6). The significant conformational changes between the molecule and its radical cation could be a main reason for these findings because this effect is not considered by the simple orbital correlation.

Conformational studies on the amidrazones including *E* and *Z* forms show that for the isolated molecules the *E* isomer is more stable than the *Z* isomer (systems **7** and **1p**) or has comparable stability (system **1q**). This is quantified by the values of the relative energies E_r of the *Z* isomers related to their *E* isomers ($E_r = 27$ kJ/mol for (*Z*)-**7**, $E_r = 34$ kJ/mol for (*Z*)-**1p** and $E_r = 0$ kJ/mol for (*Z*)-**1q**). X-ray investigations of amidrazone derivatives sometimes reveal *E* and *Z* isomers in the crystal.⁵

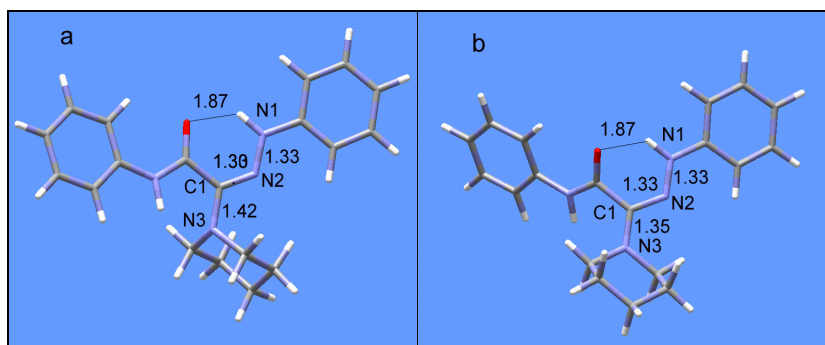


Figure 6. Calculated models of most stable structures and significant bond lengths for (*E*)-**1p** (a: neutral molecule; b: radical cation).

Moreover, the total atomic spin densities were calculated for the most stable conformers of the radical cations. It is notable that the dominant contributions were obtained at the nitrogen atoms of the amidrazone skeleton. The values at the other atoms including the C1 atom are significantly smaller. This is illustrated in Table 7.

Table 7. Significant DFT spin densities on the radical cations of amidrazones

Compound	N1	C1	N2	N3
<i>(E)</i> -7	0.419	0.035	0.133	0.142
2b	0.351	0.031	0.143	0.162
4c	0.379	0.029	0.102	0.158
8	0.348	0.0	0.172	0.260
<i>(E)</i> -1p	0.366	0.045	0.107	0.214
<i>(Z)</i> -1p	0.315	0.029	0.119	0.166
<i>(E)</i> -1q	0.363	0.033	0.141	0.177

In all cases the largest value for the total atomic spin density was found at the N1 atom, which is directly bound to the phenyl ring and most likely is the point of the radical origin. The values at the N2 and N3 atoms are comparable to a large extent excluding the radical cations of **8** and *(E)*-1p. For the *E* and *Z* isomers of 1p no remarkable change in the atomic spin density distribution was found.

Experimental Section

General Procedures. Melting points were determined on a Boetius hot-stage apparatus. NMR spectra were recorded on a Gemini 2000 and Gemini 200, operating at 399.96 MHz and 199.95 MHz for ¹H NMR and at 100.6 MHz and 50.3 MHz for ¹³C NMR spectra. TMS was used as internal standard. Chemical shifts are given in δ units and refer to the centre of the signal. Mass spectra were obtained with an AMD 402 of the firm AMD INTEDRA (70 eV). Reactions were monitored by TLC (silica gel 60 F₂₅₄, Merck) in chloroform/ether (7:3, v/v) and detected with ultraviolet light (254 nm).

Amidrazones **1a–m**, **1o–q**, triazolines **2a–i**, triazole **3a**, and benzotriazepines **4a–h** were prepared, purified and characterized as described previously.^{4,5}

(Z)-Ethyl 2-amino-2-[2-(4-chlorophenyl)hydrazono]acetate (1n). A solution of 2-ethoxy-2-oxoethane-*N*-(4-chlorophenyl)hydrazonoyl chloride (2.6 g, 10 mmol) in dioxane (~ 40 mL) was added dropwise to 7 N methanolic solution of ammonia (3.6 mL, 25 mmol). After stirring at 35 °C for at least 12 h the mixture was poured in cold water (150 mL). The solid was collected,

washed with water and dried. Recrystallization from chloroform/heptane gave pale yellow fine needles **1n** (1.4 g, 71%); mp 148–151 °C (chloroform/heptane) (lit.¹⁰ 158 °C, lit.¹¹ 144–145 °C).

Ethyl 1-(4-chlorophenyl)-1*H*-1,2,4-triazole-3-carboxylate (3b). (*Z*)-Ethyl 2-amino-2-[2-(4-chlorophenyl)hydrazono]acetate (**1n**, 2.4 g, 10 mmol), formaldehyde (37%, 1.5 mL, 20 mmol) and *p*-toluenesulfonic acid (0.1 g) were refluxed in ethanol (ca. 50 mL) for about 7 h until starting amidrazone was converted completely. The mixture was cooled to room temperature and the solvent was evaporated. The solid product was collected and recrystallized from ethanol giving white crystals **3b** (0.6 g, 24%); mp 135–136 °C (ethanol) (lit.¹² 121 °C).

Ethyl 1-(4-chlorophenyl)-5-methyl-1*H*-1,2,4-triazole-3-carboxylate (3c). Ethyl 2-amino-2-(4-chlorophenyl)hydrazonoacetate **1n** (2.4 g, 10 mmol), acetaldehyde (1.1 mL, 20 mmol) and *p*-toluenesulfonic acid (0.1 g) were refluxed in ethanol (ca. 50 mL) until the amidrazone was completely consumed. The mixture was cooled to room temperature and the solvent was evaporated. The solid product was collected and recrystallized from 2-propanol giving white crystals **3c** (0.4 g, 15%); mp 115–117 °C (2-propanol) (lit.¹³ 113–114.5 °C).

(*E*)-2-(2-Methyl-2-phenylhydrazono)-*N*-phenyl-2-(piperidin-1-yl)acetamide (7). A solution of 2-anilino-*N*-methyl-2-oxo-*N*-phenylethanehydrazonoyl chloride **6** (2.8 g, 10 mmol) in dioxane (ca. 40 mL) was added dropwise to piperidine (2.0 mL, 20 mmol) in a few mL dioxane. After stirring at 40–45 °C for at least 12 h the mixture was poured into cold water (150 mL). The solid was collected, washed with water and dried. Recrystallization from heptane gave white crystals **7** (2.3 g, 68%); mp 158–160 °C (heptane). ¹H NMR (400 MHz, DMSO-*d*₆, Me₄Si): δ 10.36 (1H, s, CONH), 6.70–7.55 (10H, Ph), 3.51 (4H, s, 2CH₂), 2.92 (3H, s, Me), 1.68 (6H, s, 3CH₂). ¹³C NMR (100 MHz, DMSO-*d*₆, Me₄Si): δ 115.2–138.1 (12C, Ph), 46.0 (1C, Me), 23.9 (1C, CH₂), 24.9 (2C; 2CH₂), 42.3 (2C, 2CH₂), 152.5 (1C, C=N), 162.3 (1C, C=O). EI-MS: *m/z* (%) 336 (80, M⁺), 84 (100). Anal. calcd. for C₂₀H₂₄N₄O: C, 71.40; H, 7.19; N, 16.65. Found: C, 71.08; H, 7.21; N, 16.39.

¹H NOE experiment (DMSO-*d*₆): Irradiation at δ 2.92 (Me), NOE at δ 6.84 (2H, Ph-H in *ortho* position of hydrazonophenyl), at δ 7.54 (2H, Ph-H in *ortho* position of anilidophenyl), and at δ 10.36 (CONH).

4-(2-Chlorophenyl)-2-phenyl-6-(piperidin-1-yl)-3,4-dihydro-1,2,4-triazin-5(2*H*)-one (8). (*Z*)-*N*-(2-Chlorophenyl)-2-(2-phenylhydrazono)-2-(piperidin-1-yl)acetamide (**1i**, 3.6 g, 10 mmol), a 37%-solution of formaldehyde (1.5 mL, 20 mmol) and *p*-toluenesulfonic acid (0.1 g) were refluxed in ethanol (ca. 50 mL) until all amidrazone was completely consumed. The mixture was cooled to room temperature and the solvent was evaporated. The solid product was collected and recrystallized from methanol to yield yellow crystals **8** (3.6 g, 92%); mp 128–130 °C. ¹H NMR (400 MHz, DMSO-*d*₆, Me₄Si): δ 6.9–7.6 (9H, Ph), 1.60 (6H, s, 3CH₂), 3.25 (4H, s, 2CH₂), 5.22 (2H, NCH₂N). ¹³C NMR (100 MHz, DMSO-*d*₆, Me₄Si): δ 114.7–145.0 (12C, Ph), 24.0 (1C, CH₂), 24.7 (2C, 2CH₂), 48.2 (2C, 2CH₂), 63.2 (1C, NCH₂N), 147.2 (1C, C=N), 152.5 (1C, C=O). EI-MS: *m/z* (%) 368 (100, M⁺). Anal. calcd. for C₂₀H₂₁ClN₄O: C, 65.12; H, 5.74; N, 15.19; Cl 9.61. Found: C, 64.93; H, 5.64; N, 15.04; Cl, 9.20.

HMBC experiment (DMSO-*d*₆): Correlation of 2H (CH₂ of triazinone) δ_H 5.22 with C=O δ_C

152.5, with C-Ph of hydrazonophenyl δ_C 145.0 and with C-Ph of anilidophenyl δ_C 136.7.

Cyclic voltammetry. Acetonitrile (Acros Organics) was of HPLC grade. Lithium perchlorate (Fluka Chemical) was used as supporting electrolyte at 0.05 M concentration in all experiments. Ferrocene (Merck KgaA, Darmstadt) was employed as inner standard at 0.01 M concentration throughout. Solutions were deoxygenated with 99,999% argon for 5 min before the start of the experiments. A platinum microelectrode (Bioanalytical Systems, diameter: 0.01 mm) and a platinum macroelectrode (diameter: 0.15 mm) were alternately used as working electrodes, together with a platinum wire auxiliary electrode and a Ag/AgCl(satd) reference electrode. At the beginning of each measurement the working electrodes had to be polished with aluminium oxide abrasive (grit size: 0.3 μm) to get comparable results. The cyclic voltammograms of the samples (conc. approx. 1 mmol in acetonitrile) were recorded at room temperature and related to Ferrocene.

Microcoulometry. 54 μmol of **2d** were dissolved in 50 ml electrolyte (0.1 M lithium perchlorate in acetonitrile) and placed in a small three-compartment-cell. The area of the platinum sheet used as working electrode was 1 cm^2 . All further instrumental parameters were the same as in the cyclovoltammetric experiment. The potential was adjusted to 700 mV and the current was registered against the time. During the electrolysis the color of the solution changed from yellow to deep blue. When the current dropped down to 0.1 mA the electrolysis was finished and the charge calculated by integration of the current along the time.

Quantum chemical calculations. Molecular and electronic structures of radical cations and their neutral molecules were investigated by the density functional theory (DFT) hybrid B3LYP method with standard 6-31G(d) basis set.⁶

Acknowledgements

Prof. Andrea Sinz is acknowledged for proof-reading the manuscript.

References

1. (a) Aly, A. A.; Nour-El-Din A. M. *ARKIVOC* **2008**, (i), 153. (b) Aly, A. A.; Gomaa, M. A.-M.; Nour-El-Din A. M.; Fahmy M. S. *ARKIVOC* **2007**, (xvi), 41.
2. Mamolo, M. G.; Zampieri, D.; Falagiani, V.; Vio, L.; Fermeglia, M.; Ferrone, M.; Pricl, S.; Banfi, E.; Scialino, G. *ARKIVOC* **2004**, (v), 231.

3. (a) Rathbone, D. L.; Parker, K. J.; Coleman, M. D.; Lambert, P. A.; Billington, D. C. *Bioorg. Med. Chem. Let.* **2006**, 16, 879. (b) Coleman, M. D.; Khan, N.; Welton, G.; Lambert, P. A.; Tims, K. J.; Rathbone, D. L. *Environ. Toxicol. Pharmacol.* **2004**, 17, 143.
4. (a) Clemens, F.; Drutkowski, G.; Wiese, M.; Frohberg, P. *Biochimica et Biophysica Acta* **2001**, 1549, 88. (b) Frohberg, P.; Kupfer, C.; Stenger, P.; Baumeister, U.; Nuhn, P. *Arch. Pharm.* **1995**, 328, 505.
5. (a) Frohberg, P.; Wagner, C.; Meier, R.; Sippl, W. *Tetrahedron* **2006**, 62, 6050. (b) Drutkowski, G.; Donner, C.; Schulze, I.; Frohberg, P. *Tetrahedron* **2002**, 58, 5317.
6. Pople, J. A. *Gaussian98*, 1998, Gaussian Inc. Pittsburg, PA.
7. Hicks, R. G. *Org. Biomol. Chem.* **2007**, 5, 1321.
8. (a) Hegarty, A. F.; Rigopoulos, P.; Rowe, J. E. *Aust. J. Chem.* **1987**, 40, 1777. (b) Rowe, J. E.; Lee, K. *Aust. J. Chem.* **1997**, 50, 849. (c) Sergutina, V. P.; Zelenin, K. N.; Khrustalev, V. A. *Zh. Org. Khim.* **1978**, 14, 622; *Chem. Abstr.* **1978**, 89, 59627. (d) Khrustalev, V. A.; Zelenin, K. N.; Sergutina, V. P. *Zh. Org. Khim.* **1979**, 15, 2280; *Chem. Abstr.* **1979**, 92, 180607.
9. Frohberg, P.; Drutkowski, G.; Wagner, C. *Eur. J. Org. Chem.* **2002**, 10, 1654.
10. Buelow, C.; Neber, P. *Ber. Dtsch. Chem. Ges.* **1913**, 46, 2041.
11. Bowack D. A.; Lapworth, A. *J. Chem. Soc.* **1905**, 87, 1859.
12. Eckert, U.; Robl, C.; Fehlhammer, W. P. *Organometallics* **1993**, 12, 3241.
13. Browne, E. J.; Polya, J. B. *J. Chem. Soc.* **1962**, 5149.